

Experimental Measures of Affine and Non-affine Deformation in Granular Shear

Brian Utter and R.P. Behringer

*Department of Physics and Center for Nonlinear and Complex Systems,
Box 90305, Duke University, Durham, NC 27708*

(Dated: November 1, 2018)

Through 2D granular Couette flow experiments, we probe failure and deformation of disordered solids under shear. Shear produces smooth affine deformations in such a solid and also irreversible so-called non-affine particle displacements. We examine both processes. We show that the non-affine part is associated with diffusion, and also can be used to define a granular temperature. Distributions for single particle non-affine displacements, δr_i , satisfy $P_1(\delta r_i) \propto \exp[-|\delta r_i/\Delta r|^\alpha]$ ($\alpha \lesssim 2$). We suggest that the shear band forms due to a radially outward diffusive flux/non-affine motion which is balanced in the steady state by inward diffusion due to density gradients.

The way in which disordered solids undergo plastic i.e. irreversible deformation is a topic of considerable recent interest[1, 2, 3, 4, 5, 6, 7, 8], in part, because the phenomena appear to be general across a large collection of materials that include glasses, foams, colloids and granular materials, among others. Here, we focus on granular materials. Despite a variety of experiments on bulk deformation of granular materials, the microscopic basis for plasticity remains elusive. Molecular dynamics simulations[2, 3, 4, 5, 6] have provided some insight, although a number of these studies involve particles that interact via frictionless forces. At this point, there is relatively little experimental work that directly addresses the connection between the microscopic and larger scale nature of granular plasticity. The goal of the present work is to begin to fill this void.

There is, however, a relatively extensive literature that considers microscopic plastic deformation in amorphous molecular solids[3, 4, 5, 6]. In the limit of low temperatures where thermal noise is irrelevant, it is expected that the plastic behavior in such materials is similar to what occurs in a granular materials. Both microscopic and granular materials exist in disordered jammed states, and when sheared, undergo irreversible configurational changes. In the granular case, the configurational structures also involve force chains, long filamentary structures that form so as to resist shear, e.g. Fig. 1.

In recent theoretical work, Falk and Langer (FL)[1] developed models of elasto-plastic deformation of amorphous solids which have also been applied recently to granular materials [7, 8]. FL consider localized regions that are susceptible to irreversible failure. Associated with any smooth affine structural change or deformation in such a region, there is a non-affine part which leads to irreversibility/plasticity. In their analysis, FL [1] consider small clusters of N particles. They fit local deformations occurring over a time Δt to an affine deformation. To identify localized plastic rearrangements, they define a quantity (D_{min}^2) which characterizes departures from the local affine deformation.

In this letter, we characterize the motion generated in 2D granular Couette (shear) flow in terms of affine and non-affine components. For this system, deformation is

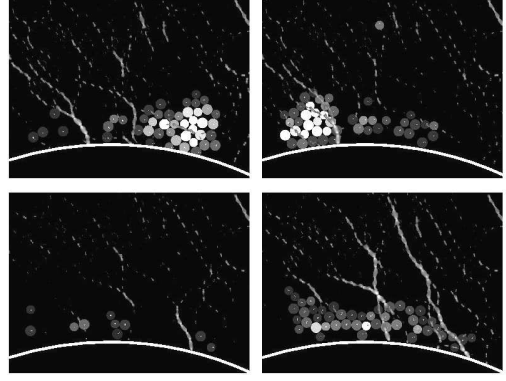


FIG. 1: Time sequence of images emphasizing the spatially inhomogeneous and temporally intermittent nature of force chains (bright lines) and active areas of non-affine deformation (shaded disks). Each disk shows a local instantaneous value for D_{min}^2 (see text), where brighter corresponds to larger D_{min}^2 . Images are separated in time by $5\Delta t$ (see text), and run left-to-right, top-to-bottom. The shearing wheel, located near the bottom of each image, rotates counterclockwise. Normally black, the edge of the wheel is highlighted for visibility.

localized to a shear band of width less than 10 grain diameters. Despite the relatively rapid variation of quantities with radial distance, it is still possible to characterize the local affine and non-affine components of the flow. However, there are some differences, discussed below, between the case of homogeneous pure shear studied in FL, and the present case, which is spatially varying and also involves rotation of small volume elements.

The experimental apparatus used here and described in greater detail elsewhere[9], is a 2D Couette shearing experiment. A dense packing of $\sim 45,000$ bidisperse photoelastic disks lie on a flat horizontal surface. In that plane, the disks are bounded by an inner shearing wheel and an outer concentric ring. The wheel rotates slowly ($f = \text{inverse rotation period} = 1\text{mHz}$ in the present experiments) to impose quasistatic shear. Particles are marked with lines for easier tracking of position and rotation. The apparatus is illuminated from below and imaged from above by two cameras. One camera observes the grains through crossed polarizers while the

other simultaneously takes unpolarized images. In this way, we record both stresses (through photoelastic measurement with polarized images) and kinematic information (by particle tracking with unpolarized images). We note that the motion is confined to a shear band near the shearing wheel. The tangential velocity $v(r)$ and local shear rate $\partial v / \partial r$ decrease faster than exponentially with radial distance from the shearing surface and have fallen by three orders of magnitude from their value at the shearing wheel for $r \gtrsim 8d$ [10]. Here, we choose $r = 0$ to correspond to the surface of the shearing wheel. In addition to the radial velocity gradient, there is also a density gradient, i.e. Reynolds dilatancy. The density/packing fraction near the wheel can be lower by as much as $2/3$ of the density far away.

In order to characterize the motion, we consider localized regions falling within $2.2d$ of a reference particle, where d is the mean particle diameter. (FL use a similar sampling radius of $2.5a_{SL}$ where a_{SL} is an interatomic distance.) Typically, we find $N \simeq 15$ particles in such a neighborhood, including the particle of interest. We then follow the motion of these N particles over a time $\Delta t = 1.85s$ that is short compared to $1/f$. We are interested in the deformation of this patch. To this end, we determine the location of each particle relative to the patch center of mass (CoM), both initially (r_i), and after the small elapsed time (r'_i). We determine the smooth mapping that best describes the affine deformation, by least squares fitting data for the r_i and r'_i in a cluster to the form $r'_i = \mathbf{E}r_i$, where \mathbf{E} is a 2×2 matrix. $D_{min}^2 = \Sigma(r'_i - \mathbf{E}r_i)^2$ is the parameter of Falk and Langer, with the slight modification that we must consider motion relative to the CoM, since there is net flow in our system. \mathbf{E} is in general not symmetric, and hence its eigenvalues may be (and often are) complex. This is a consequence of the typical deformation in the present flows: on average, there is both deformation of a volume element, characterized by a symmetric tensor, \mathbf{F} , and rotation, characterized by a rotation tensor, \mathbf{R}_θ . This differs from the case of pure shear, where there is no rotation on average. We write $\mathbf{E} = \mathbf{R}_\theta \mathbf{F}$ without serious ambiguity. For instance, inverting the order of \mathbf{F} and \mathbf{R}_θ does not change θ or the eigenvalues of \mathbf{F} . Also, θ is uniquely determined if we restrict $-\pi/2 < \theta \leq \pi/2$, which is not an issue for the small deformations considered here. We can then express the deformation in terms of the eigenvalues, ϵ_i , of $\epsilon = \mathbf{F} - \mathbf{I}$, where ϵ is the conventional strain tensor, and \mathbf{I} is the unit tensor. Together with θ , they characterize the affine part of the local evolution. D_{min}^2 characterizes the extent of the nonaffine motion for the small region in question. We note that all measures of the deformation, both affine and non-affine are spatially and temporally intermittent, as seen for instance in Fig. 1. Hence, it is important to consider the probability distribution functions (PDF's) of these measures as functions of r .

We first consider data for the affine deformations. In Fig. 2 we show PDF's for the eigenvalues of ϵ , which we

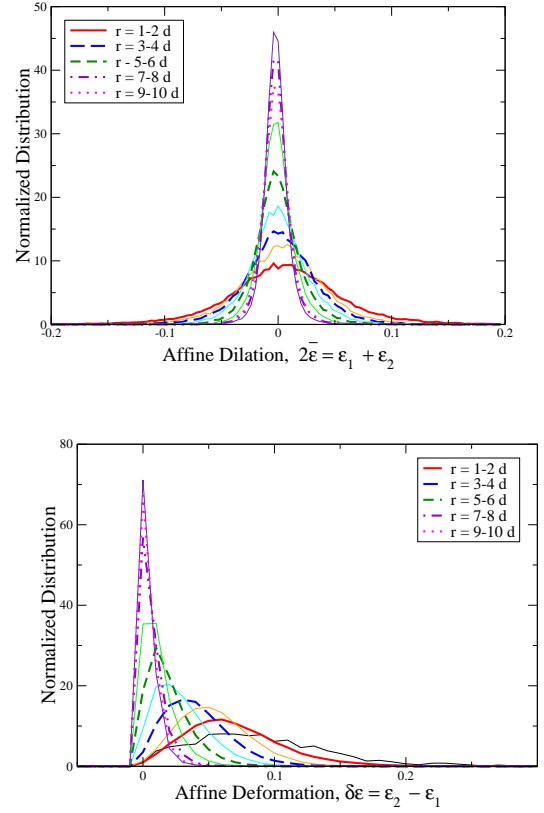


FIG. 2: PDF's of the affine dilation, $\epsilon_1 + \epsilon_2$ (top), and affine shear deformation, $\epsilon_2 - \epsilon_1$ (bottom). Each series corresponds to a radial bin of width d . The notation $r = 1 - 2d$, etc. indicates that the central particle of the cluster was located radially between d and $2d$ from the wheel, etc.

give in the form $\delta\epsilon = \epsilon_2 - \epsilon_1$ and $2\bar{\epsilon} = \epsilon_1 + \epsilon_2$. The different data sets in each figure are binned over radial widths of size d , and correspond to a series of radial distances, each d apart, from the shearing wheel. The first series is centered at $d/2$ from the shearing wheel. We expect that $\bar{\epsilon}$ has zero mean in the steady state, since it corresponds to the dilation of the local patches; $\delta\epsilon$ has non-zero mean and a characteristic shape that reappears in the data for D_{min}^2 , discussed below. PDF's for θ resemble those for $\delta\epsilon$; mean values for θ are typically a few degrees or less.

We plot the PDF's of D_{min}^2 binned at different distances r from the shearing surface in Fig. 3(top). The peak in the PDF of D_{min}^2 tends to be at larger values of D_{min}^2 for r closer to the shearing wheel, although the position of the peak does not vary monotonically with r , a point that we consider below. The individual PDF's are well fitted by the form $f(x) = C_1 x^{C_2} e^{-x/C_3}$, which we discuss further below. However, the exponent C_2 and the scaling factor C_3 in the exponential vary from fit to fit. In Fig. 3(bottom), each of the data sets is rescaled in the vertical direction by the peak fit value and in the horizontal direction by the mean $\langle D_{min}^2 \rangle$. We see that the data at different r collapse fairly well onto a single curve. The averages $\langle D_{min}^2 \rangle$ (inset), are set by the local shear rate

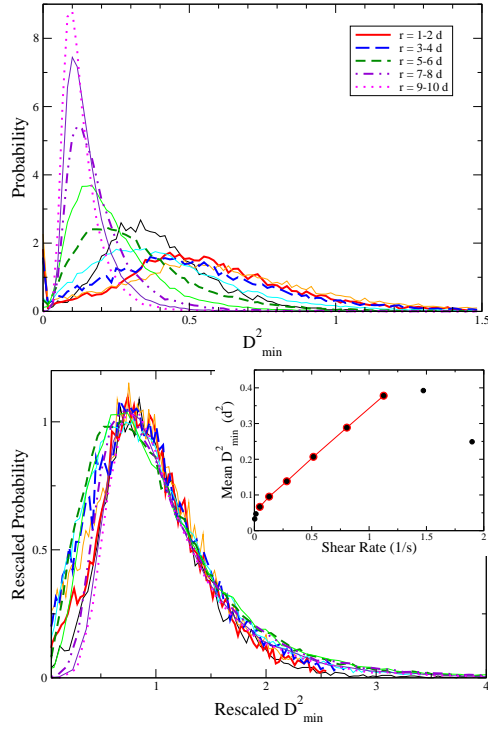


FIG. 3: Top: PDF's of D_{min}^2 (units of d^2) at various distances r from the shearing surface (in units of d) for 1080 images. Bottom: Rescaled data from top. Each data set is fitted and rescaled by the peak magnitude and mean value of D_{min}^2 . Inset: $\langle D_{min}^2 \rangle$ vs. local shear rate. Note the drop in $\langle D_{min}^2 \rangle$ (departure from red line) at high $\dot{\gamma}$, i.e. near wheel.

within the shear band (inset, bottom). We previously observed a similar dependence for diffusivity, D , on local shear rate $\dot{\gamma}$, i.e. $D \propto \dot{\gamma}$ [9]. In Fig. 4, we plot $\langle D_{min}^2 \rangle$ and radial and tangential diffusivities (D_{rr} and $D_{\theta\theta}$) rescaled such that all quantities are 1 at $r = 2d$. The diffusivity is therefore proportional to the mean measure of local plastic rearrangements $\langle D_{min}^2 \rangle$. It is perhaps not surprising that diffusivity and D_{min}^2 are related, as they both measure non-affine displacements. Dimensionally, D_{min}^2 has units of x^2 and is measured over a specified time interval Δt . Diffusivity D is set by $D \sim \langle (\Delta x)^2 \rangle / \Delta t$. In these experiments, displacements scale by some fraction of d over times scales of order the local inverse shear rate $\dot{\gamma}^{-1}$, e.g. $D \sim \dot{\gamma} d^2$ and $D_{min}^2 \sim \dot{\gamma} \Delta t d^2$.

The decrease in diffusivity and $\langle D_{min}^2 \rangle$ for $r \approx 0$ in Fig. 4 results from several effects. Particles in contact with the shearing surface are dragged quasi-ballistically in the azimuthal direction[9]. In addition, radial diffusion is limited to the outward direction next to the shearing wheel. Roughly, one might expect a decrease by 1/2 for particle variances for radial displacements (and hence radial diffusivity, D_{rr}) near the wheel.

D_{min}^2 is a mesoscopic property, i.e. a locally averaged measure of a grain-scale process. The scaling property observed for the PDF's of D_{min}^2 suggest that there may

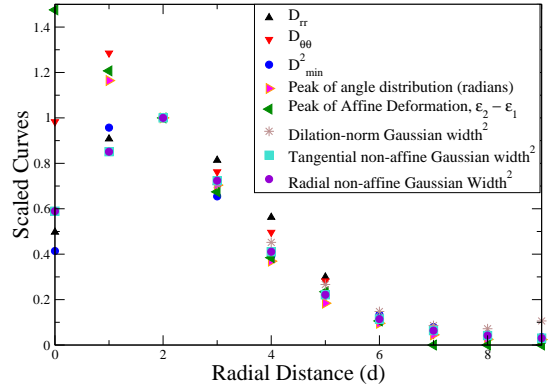


FIG. 4: Rescaled $\langle D_{min}^2 \rangle$, widths of non-affine PDF's, $P_1(\delta \mathbf{r}_i)$, diffusivities, and peak values of $P(\theta)$ and $P(\epsilon_2 - \epsilon_1)$ versus radial distance from the shearing wheel. All quantities are scaled to 1 at $r = 2d$. For reference, at $r = 2d$, $\dot{\gamma} = 0.60 s^{-1}$, $D_{rr} = 0.0054 d^2/s$, $D_{\theta\theta} = 0.011 d^2/s$, $\langle D_{min}^2 \rangle = 0.38 d^2$, $\theta_{peak} = 0.045 rad$, $(\epsilon_2 - \epsilon_1)_{peak} = 0.047 d$. Square widths for other PDF's are: $P(\epsilon_2 - \epsilon_1) - 0.0016 d^2$, $(P_1(\delta \mathbf{r}_i) - -radial)^2 - 0.0050 d^2$, $(P_1(\delta \mathbf{r}_i) - -azimuthal) - 0.0053 d^2$.

be an underlying microscopic phenomena of interest. To this end, we examine in Fig 5 (top), the PDF's $P_1(\delta \mathbf{r}_i)$ of the individual non-affine particle displacements, $\delta \mathbf{r}_i = \mathbf{r}_i' - \mathbf{E} \mathbf{r}_i$. The PDF for P_1 is approximately gaussian, $P_1(\delta \mathbf{r}_i) \simeq A \exp[-(\delta \mathbf{r}_i / \Delta r)^\alpha]$, where $\alpha \leq 2$. To see this, we plot in Fig. 5 (middle), $\log|\log(P_1(\delta \mathbf{r}_i))|$ as a function of $\log(\delta \mathbf{r}_i)$, with P_1 normalized so that $P_1(0) = 1$. These data are striking in as much as they resemble the velocity distributions for granular gas-like states[11, 12], even though the basic kinetic theory assumption of short-lived uncorrelated collisions/contacts is manifestly violated. Interestingly, PDF's for the *total* displacements, $\mathbf{r}_i' - \mathbf{r}_i$, are exponentially distributed, Fig 5 (bottom).

D_{min}^2 is constructed by choosing N particles in a cluster, and then computing $D_{min}^2 = (\sum_N \delta \mathbf{r}_i^2)$. The PDF for D_{min}^2 , constructed from clusters of N particles is

$$P(D_{min}^2) = \int P_N(\delta \mathbf{r}_1, \dots, \delta \mathbf{r}_N) \delta(D_{min}^2 - \sum (\delta \mathbf{r}_i)^2) d\delta \mathbf{r}_1 \dots d\delta \mathbf{r}_N, \quad (1)$$

where P_N gives the PDF for the N non-affine particle displacements. We do not *a priori* know $P_N(\delta \mathbf{r}_1, \dots, \delta \mathbf{r}_N)$. However, if we assume that the individual particle displacements are uncorrelated and given by gaussian PDF's: $P_1(\delta \mathbf{r}_i) = B \exp[-(\delta \mathbf{r}_i / \Delta r)^2]$, then the above integral for the PDF for D_{min}^2 follows with a bit of algebra. (Although neither of these assumptions is rigorously true, neither is markedly unreasonable.) Then, $P(D_{min}^2) = C_1 (D_{min}^2)^{N-1} \exp(-D_{min}^2 / C_2)$, where the C_i are constants. This form is qualitatively consistent with the experimentally obtained PDF's for D_{min}^2 (Fig. 3). Applying this strictly is probably not warranted, since some correlation is likely, and the measured P_1 's are not truly gaussians.

The widths of the $P_1(\delta \mathbf{r}_i)$ (Fig. 4) can be taken as an effective granular temperature associated with the non-

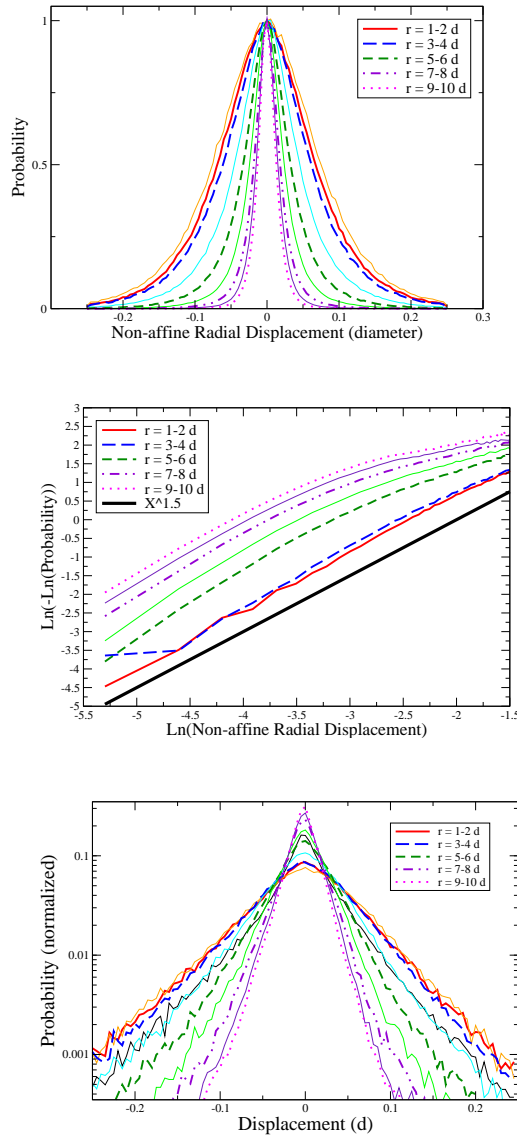


FIG. 5: Data for individual particle non-affine radial displacements, $P_1(\delta r_i)$. Top: on linear scales, Middle: on log-log scales (solid black line shows slope 3/2). PDF's for the non-affine azimuthal displacements are similar. Bottom: PDF's of total displacements, $r'_i - r_i$, on log-lin scales.

affine/diffusive displacements of the particles (hence presumably a configurational measure). However, we give a note of caution here concerning the relation of this temperature to the overall energy in the system. The elastic energy and elastic energy fluctuations for this system are several orders of magnitude larger than the corresponding kinetic energies associated with both the affine and non-affine motion. In addition, the motion considered here is driven by the wheel displacement, not its velocity. If the experiments were slowed by any amount, the basic phenomena would appear essentially the same when expressed in terms of displacements.

In closing we offer the following insight into the formation of a shear band from an initially homogeneous state. Both the affine and non-affine motion are driven by and extract energy from the wheel displacement and the stored elastic energy. Non-affine deformation is associated with diffusive motion, whose source is the stirring from the wheel. When the wheel begins to turn, there is a radially outward flux driven by the excitation of the shearing wheel (there can be no inward diffusion there). This flux is the source of the (Reynolds) dilation next to the wheel. Such a flux is diffusive in the steady state, and is then counterbalanced by the resulting gradients of density/free volume which cause a compensating reverse mass flux. This state is also mechanically stable due to the reduction in density and contact number near the wheel. The system is less resistant to shear near the wheel due to contact number depletion, leading to localization of motion. In the present system, which has a fixed volume, one expects an increase in density outside the dilated region, which tends to limit the growth of the shear band, in contrast to recent 3D experiments[13] with an open top where the growth of the shear band is much less constricted. An interesting question is the extent to which similar phenomena occur in other disordered solids.

Acknowledgment We appreciate helpful discussions with A. Lemaitre and J. Langer, and comments from B. Chakraborty and M. Sperl. This work has been supported by the NSF grants DMR-0555431, DMS-0204677 and DMS-0244492, and NASA grant NAG3-2372.

-
- [1] M. Falk and J. Langer, Physical Review E (Statistical Physics, Plasmas, Fluids, and Related Interdisciplinary Topics) **57**, 7192 (1998).
 - [2] S. Luding, J. Phys.:Condens. Matter **17**, S2623 (2005).
 - [3] C. Maloney and A. Lemaitre, Phys. Rev. Lett. **93**, 016001 (2004).
 - [4] C. Maloney and A. Lemaitre, Phys. Rev. Lett. **93**, 195501 (2004).
 - [5] M. J. Demkowicz and A. S. Argon, Phys. Rev. B **72**, 245206 (2005).
 - [6] F. Leonforte, R. Boissière, A. Tanguy, J. P. Witmer, and J.-L. Barrat, Phys. Rev. B **72**, 224206 (2005).
 - [7] A. Lemaitre, Physical Review Letters **89**, 064303 (2002).
 - [8] A. Lemaitre, Physical Review Letters **89**, 195503 (2002).
 - [9] B. Utter and R. P. Behringer, Phys. Rev. E **69**, 031308 (2004).
 - [10] B. Utter and R. P. Behringer, Euro. Phys. J. E **14**, 373 (2004).
 - [11] F. Rouyer and N. Menon, Phys. Rev. Lett. **85**, 3676 (2000).
 - [12] W. Losert, D. G. W. Cooper, J. Delour, A. Kudrolli, and J. P. Gollub, Chaos **9**, 682 (1999).
 - [13] D. Fenistein, J. W. van de Meent, and M. van Hecke, Phys. Rev. Lett. **92**, 094301 (2004).